Ionization and double excitation of helium by short intense laser pulses

Armin Scrinzi[1] and Bernard Piraux[2]

[1]*Institut für Theoretische Physik, Universität Innsbruck, Technikerstrasse 25, A-6020 Innsbruck, Austria*

[2]*Institut de Physique, Université Catholique de Louvain, 2, Chemin du Cyclotron, B-1348 Louvain-la-Neuve, Belgium*

(Received 17 March 1997)

We present an *ab initio* calculation of single ionization, harmonic generation, and double excitation of helium by short (3.8–15.2 fs) moderately strong (peak intensity 1.49×10^{14} W/cm^2) laser pulses with wavelengths between 40 and 152 nm. We find excitation to be dominated by resonances with bound and doubly excited states. The processes are nonperturbative. The finite pulse duration leads to resonance broadening and far-off-resonant transitions. [S1050-2947(97)50107-7]

PACS number(s): 32.80.Rm, 32.80.Fb

The field strengths of laser pulses that are routinely used in experiments approach and in some cases surpass the atomic field strength. Such high fields may be obtained with pulses whose duration is less than 100 fs. A theoretical interpretation of experiments under such conditions requires a nonperturbative and nonstationary description of the laser-atom interaction. Experimentally observed single electron and harmonic spectra are in good agreement with computations employing the single active electron (SAE) description of the atom, where only one electron interacts with the field and effective potentials replace the core electrons [1,2]. The SAE model provides a computationally fast and simple description of the atom that allows to study all dominantly single-electron properties of the atom in a wide range of frequencies and intensities. The interest in going beyond that picture is twofold: first, to provide an independent check of the SAE model, and second, to be able to describe genuine two-electron phenomena like double excitation or (nonsequential) double ionization.

The first insight into two-electron effects in laser-atom interaction was gained by one-dimensional models of a two-electron atom [3,4], in which the angular degrees of freedom are suppressed. One limitation of such models is that they do not, in general, have a realistic atomic bound-state spectrum. A second, possibly more serious limitation is the absence of angular momentum in a process where angular-momentum selection rules play an important role. There are three major efforts for a complete three-dimensional description of He in a nonperturbative laser field: One approach employs a grid discretization of space and the distribution of angular momentum over the processors of a massively parallel machine [5]. In these calculations the Coulomb potential between the two electrons is restricted to one single or a few multipole terms in order to reduce interprocessor communication and the spatial grid is very coarse ($\sim$0.5 a.u.) to retain manageable computation times. Consequently, atomic states are only approximately described. A second group combines elaborate atomic structure programs with Floquet theory [6]. This approach can provide realistic results for a larger variety of atomic species at field parameters, where the atomic structure is not too severely disturbed. Floquet theory limits the application to long, slowly varying pulses. Finally, a dedicated two-electron program is pursued in Ref. [7]. There correlated two-electron functions are obtained by combining numerical single-electron functions. In the spirit of atomic physics the angular electron correlation is described by the proper combination of single-particle spherical harmonics. Very detailed results for photoelectron spectra could be obtained with this method.

In this paper we present results on ionization and single and double excitation of helium exposed to short laser pulses with realistic pulse durations of 157 to 628 a.u. ($\sim$3.8–15.2 fs) and intermediate peak intensities of 0.004 23 a.u. (1.49×10^{14} W/cm^2). Frequencies range from 0.3 to 1.15 a.u., which corresponds to wavelengths from 151.8 to 39.6 nm. The results are obtained by direct time-integration of the Schrödinger equation without any approximations except for the dipole approximation of the laser field. In the velocity gauge the Schrödinger equation reads

$$i\frac{d}{dt}\Psi(\vec{r}_1,\vec{r}_2;t)=\left[-\frac{1}{2}(\Delta_1+\Delta_2)+\frac{i}{c}\vec{A}(t)\cdot(\vec{\nabla}_1+\vec{\nabla}_2)-\frac{2}{r_1}-\frac{2}{r_2}+\frac{1}{|\vec{r}_1-\vec{r}_2|}\right]\Psi(\vec{r}_1,\vec{r}_2;t), \tag{1}$$

where $\vec{r}_1$ and $\vec{r}_2$ are the electron coordinates measured from the nucleus and Δ_i and $\vec{\nabla}_i$ are the corresponding gradient and Laplace operators. We use linearly polarized pulses of duration T with a $\sin^2$-shaped envelope of the vector potential $\vec{A}$,

$$\vec{A}(t)=\sin^2(\pi t/T)\sin(\omega t)(0,0,A_0). \tag{2}$$

To avoid reflections in the finite range of space that can be numerically represented we use the method of complex scaling. This method can be viewed as a systematic way of implementing outgoing wave boundary conditions. (For an intuitive discussion, see Ref. [8].) It consists of analytically continuing the Hamiltonian by multiplying the real coordinates by a complex number

$$H(\vec{r}_1,\vec{r}_2;t)\rightarrow H_\theta=H(e^{i\theta}\vec{r}_1,e^{i\theta}\vec{r}_2;t), \tag{3}$$

where the scaling angle θ is real. The new Hamiltonian H_θ has the same bound-state spectrum as H, doubly excited states appear as square integrable eigenfunctions with com-

plex eigenvalues, where the imaginary part gives 1/2 of the autoionization width, and the continuous spectrum is rotated into the lower half plane. We time integrate Eq. (1) using the complex scaled H_θ in place of H. Contrary to the time-independent case, to our knowledge, there is no mathematically rigorous theory to interpret the results of the complex scaled time propagation. It is, however, known that the projections on the complex scaled bound and doubly excited states have θ independent meaning as the populations of the respective physical states. We therefore interpret these projections as physical quantities. Their numerical independence of θ provides an important accuracy check for our calculations. Similarly, the harmonic spectrum extracted from the complex scaled wave function is taken to be physical within the accuracy determined by its variation with θ.

For the discretization of Eq. (1) we expand Ψ in a Hylleraas-like explicitly correlated basis

$$\Psi(\vec{r}_1,\vec{r}_2;t)=\frac{1}{2}(1+P_{12})\sum_{L=0}^{L_{\max}}\sum_{l_1=0}^{L} G_{Ll_1}(\vec{r}_1,\vec{r}_2) \times\sum_i c_i^{Ll_1}(t) r_1^{k_i} r_2^{m_i} |\vec{r}_1-\vec{r}_2|^{n_i} \times\exp(-\alpha_i r_1-\beta_i r_2). \quad (4)$$

The operator $(1+P_{12})/2$ projects on the singlet states. The two-electron angular factors G_{Ll_1} for total angular momentum L and z component $L_z=0$ are

$$G_{Ll_1}=r_1^{l_1} r_2^{L-l_1}\sum_m C^{L,0}_{l_1,m;L-l_1,-m} Y^{l_1}_m(\hat{r}_1) Y^{L-l_1}_{-m}(\hat{r}_2). \quad (5)$$

The $C^{L,0}_{l_1,m;L-l_1,-m}$ are Clebsch-Gordan coefficients and Y^l_m are spherical harmonics. For each (L,l_1) several sets of exponents (α_i,β_i) were used and the combination of powers (k_i,m_i,n_i) was constrained in a way as described in Ref. [9]. Note that for each L there are only $L+1$ angular functions G_{L,l_1}. Angular correlation, which in the usual atomic physics basis requires a large number of combinations of single-electron angular momenta l_1 and l_2, is here contained in the interelectron coordinate $|\vec{r}_1-\vec{r}_2|$. It has been demonstrated that such a basis is capable of efficiently and accurately representing He bound states [9,10]. In the time propagation we used an average of 300 expansion functions for each L between 0 and $L_{\max}=7$. Our discretized atomic Hamiltonian matrix contained six to eight bound states for each L, out of which the lowest three to four had an accuracy in energy of $\lesssim 10^{-8}$ a.u. The energies and widths of the lowest doubly excited states as obtained with that basis are compared in Table I with literature values.

The time integration of the discretized equation was performed with a sixth-order seven-stage explicit Runge-Kutta method. The error was controlled by comparing every two integration steps with a single double-step size integration. For a few frequencies stability was verified with an implicit Runge-Kutta scheme.

Figure 1 shows the probability of excitation and ionization of He by pulses of duration $T=157$ a.u. (3.8 fs). The total pulse energy

TABLE I. Energies and widths of doubly excited states as obtained with the basis used for time propagation compared to literature values. The states given are the lowest below the $He^+(n=2)$ and $He^+(n=3)$ ionization thresholds, respectively, for angular momenta $L=0,\ldots,4$. All states are singlet with parity $(-1)^L$.

	Present		Literature	
L	E	Γ	E	Γ
0	-0.777 80	4.45×10^{-3}	-0.777 868	4.53×10^{-3} [a]
0	-0.353 56	3.004×10^{-3}	-0.353 537	3.004×10^{-3} [a]
1	-0.693 12	1.345×10^{-3}	-0.693 134 9	1.3733×10^{-3} [a]
1	-0.335 53	6.7×10^{-3}	-0.335 625 9	7.023×10^{-3} [a]
2	-0.701 92	2.44×10^{-3}	-0.701 945 7	2.3622×10^{-3} [a]
2	-0.343 02	5.30×10^{-3}	-0.343 173	5.155×10^{-3} [a]
3	-0.558 28	1.17×10^{-5}	-0.558 28	1.28×10^{-5} [b]
3	-0.304 19	3.30×10^{-3}	-0.304 215	3.25×10^{-3} [a]
4	-0.532 36	9.64×10^{-6}		
4	-0.310 42	6.84×10^{-3}	-0.307 05	6.70×10^{-3} [a]

[a]Ho *et al.*, as tabulated in Ref. [11].
[b]Lindroth, Ref. [11].

$$W=\int_0^T dt\left(\frac{1}{c}\frac{\partial\vec{A}}{\partial t}\right)^2 \quad (6)$$

is kept constant at $W=0.5$ a.u., which corresponds to a peak intensity of $\approx 0.004\,23$ a.u. $=1.49\times10^{14}$ W/cm^2. In the absence of resonance there is no significant population of the bound states and excitation goes primarily into the continuum. There is a range of two-photon resonances around the frequency $\omega=0.4$. The most prominent of these resonances occurs at $\omega=0.38$ with the first excited S state of energy -2.1460 a.u., where the excitation yield reaches 5% at ionization of only 1%. The second group are the single-photon resonances between $\omega=0.7$ and the single-photon ionization threshold. They are dominated by the 2^1P^o bound state (energy $-2.123\,84$ a.u.) with a resonance frequency of $\omega=0.78$ a.u. We checked that the dip seen in the bound-state excitation at $\omega=0.72$ is due to a Rabi-type oscillation between the ground state and the lowest P state. It is therefore very sensitive to intensity and pulse duration an will be smeared out in an experiment.

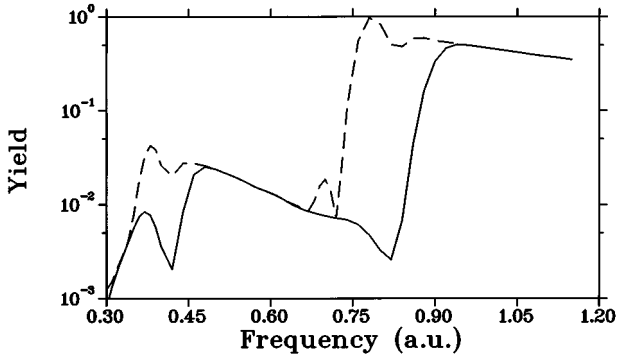

FIG. 1. Single excitation and ionization from the ground state of He by $\sin^2$-shaped pulses of duration $T=157$ a.u. and pulse energy $W=0.5$ a.u. Lower curve, ionization yield; upper curve, sum of ionization and excitation.

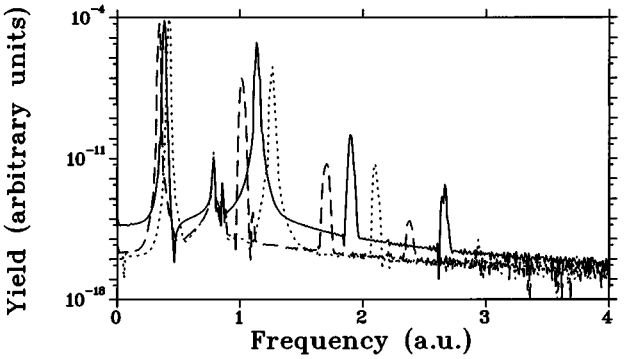

FIG. 2. Harmonic generation by pulses of energy $W=0.5$ and duration 628 a.u. at frequencies $\omega=0.34$ (dashed line), 0.38 (solid line), and 0.42 a.u. (dotted line).

The resonance at $\omega=0.38$ is also reflected in an enhanced polarizibility and a corresponding enhancement of harmonic generation. In Fig. 2 one can compare the harmonic spectra at laser frequencies $\omega=0.34$, 0.38, and 0.42. The relative enhancement at $\omega=0.38$ is clearly visible. When one projects out the first excited S state the harmonic yields decrease by 1 to 2 orders of magnitude and become comparable with the yields off resonance. The structure between the first and third harmonic is due to transition from excited P states to the ground state.

We now turn to the genuine two-electron process of double excitation. Figure 3 depicts the total population remaining after passage of the $T=157$ a.u. pulse in all doubly excited states that can be unambiguously represented by our basis. Like for the bound states, a clear resonance structure is discernible. Due to the short duration of the pulse, the various resonances overlap. The five broad peaks crudely correspond to six-, five-, four-, three-, and two-photon transitions to the doubly excited states with even and odd angular momenta, respectively. The dominant contributions to the doubly excited population are made by the lowest states. In Fig. 4 we show the population of the lowest doubly excited D state. Comparing the heights of the peaks in Figs. 3 and 4 one sees that on resonance the state completely dominates the doubly excited population. The three sharper peaks are the six-photon ($\omega=0.37$) and four-photon ($\omega=0.55$) and two-photon ($\omega=1.10$) resonances. Their widths are due to

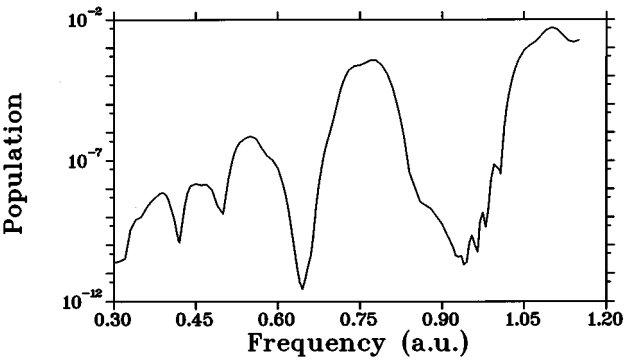

FIG. 3. Populations in the doubly excited states of He after passage of a pulse of duration 157 a.u. and pulse energy $W=0.5$ a.u.

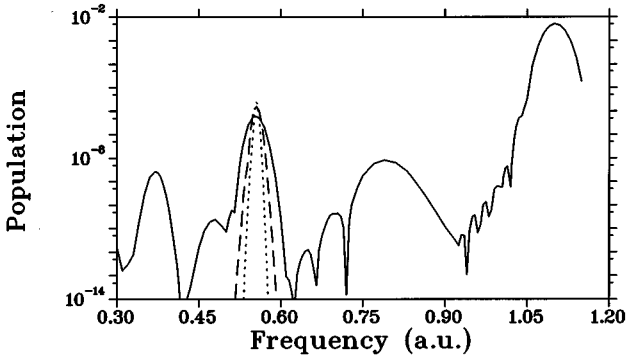

FIG. 4. Populations in the lowest doubly excited D state. Solid line, pulse duration $T=157$ a.u. and pulse energy $W=0.5$; dashed line, $T=314$, $W=1$; dotted line, $T=628$, $W=2$.

the bandwidth of the pulse. Longer pulses lead to narrower peaks, as demonstrated in Fig. 4 for the four-photon resonance. The broad quite unexpected structure between $\omega=0.7$ and $\omega=0.9$ closely mirrors the population of the 2^1P^o state, which is one-photon resonant in this frequency range. We found that the ratio between the P-bound and D-doubly excited population is proportional to intensity and can therefore be ascribed to a first-order far-off-resonant transition from P to D with a transition energy 1.422 a.u. Such a transition is allowed because of the bandwidth of the pulse. When we increase the pulse duration, the effect quickly diminishes. The transition is strongest for the doubly excited D state, but occurs also for the other bound and doubly excited states of even symmetry.

We investigated the convergence of our calculations with respect to the basis size for each angular momentum, the maximum included angular momentum $L_{\max}$, and the complex scaling angle θ. Convergence strongly depends on the frequency. Single excitation and ionization are converged within $\lesssim 5\%$ in the whole range of frequencies. The double excitation peaks at the frequencies $\gtrsim 0.5$ a.u. are similarly accurate. In fact, the two-photon peak is already well reproduced using $L_{\max}=2$, which shows that Raman transitions to the doubly excited state play no role at these frequencies. Below $\omega\approx 0.5$ a.u., convergence of the doubly excited populations becomes increasingly harder to achieve. The necessary $L_{\max}$ rapidly rises and at $\omega=0.3$ we reach the limit of what we consider sensible results for double excitation with $L_{\max}=7$. We estimate that the lowest double excitation peak in Fig. 4 is only accurate to within a factor $2\sim 3$. This includes both the dependence on the scaling angle θ and angular-momentum truncation. The size of the basis at a given angular momentum is less critical. The harmonic spectra depend on the details of the wave function and are therefore relatively more sensitive to basis size and scaling angle. We estimate that the heights of all peaks seen in Fig. 2 are accurate within $\pm 50\%$.

On the whole, the doubly excited populations are small when compared to the ionization yields and the question of their observability arises. It appears unlikely that the very weak fluorescence from doubly excited states can be observed, since due to the short lifetime of the most strongly populated states it would have to be observed on the background of harmonics generated by the laser. Fluorescence is

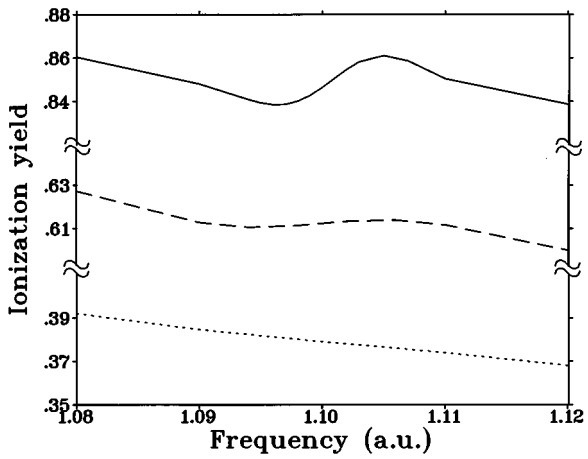

FIG. 5. Total ionization yield around the two-photon resonance to the lowest doubly excited D state. The curves from bottom to top are for pulse duration $T=157$, 314, and 628 a.u. and pulse energies $W=0.5$, 1, and 2 a.u., respectively.

also suppressed, because the states decay predominantly by autoionization with a state-dependent branching ratio of the order 1:1000.

Another possibility is to observe the interference between the alternative paths of direct photoionization and double excitation with subsequent autoionization. In Ref. [6] a pronounced Fano profile was reported for the ionization rate when passing the two-photon resonance frequency. The visibility of this structure is limited by the bandwidth for short pulses. Figure 5 shows the yield for pulses of duration 157, 314, and 628 a.u. with constant peak intensity of 1.49 a.u. The modulation of the yield varies from the hardly visible for the shortest pulses, over a variation of $\approx 1\%$ for the intermediate to about 2.5% at the longest pulse, where ionization reaches 85%. The modulations of the *total* yield are small, but when photoelectron energies are resolved, a very clear signature of the interference can be found. For example, at pulse duration $T=314$ we estimate by comparison with a hydrogenlike ion that only about 1% of the total photoelectrons are contained in the two-photon ionization peak that is subject to the interference. A change of the order 1% in total yield means that the height of the two-photon photoelectron peak changes drastically.

Nonperturbative effects manifest themselves in the dependence of the height of the double excitation peaks on the pulse energy W. When we parameterize the dependence of the peak heights by $P \propto W^{\kappa}$ we find that κ depends on W. For the six-photon peak the exponent varies between $\kappa=5.5$ at $W=0.1$ and $\kappa=4.3$ at $W=0.5$, while at the four-photon peak the variation is between $\kappa=3.9$ and 3.6.

We would like to emphasize that on account of the accurate description of the bound and doubly excited-state spectrum of helium we consider our results quantitatively reliable within the basis set truncation error indicated above. This estimated error is below about 5% for large part of the data. The single excitation and ionization data presented here should be compared to the results of SAE calculations. There is no published data for the given range of parameters, but the differences for the predominantly single-electron processes may be small. We expect the accuracy of an SAE calculation for the given parameters to mostly depend on the accuracy of its bound-state spectrum and ionization potential. The *ab initio* calculation of double excitation of helium by short laser pulses presented here shows that already at the relatively moderate intensities used in the calculations significant nonperturbative effects appear. The time dependence of intensity leads to resonance broadening and the appearance of far-off-resonant transitions.

We wish to thank Robin Shakeshaft and Marcel Pont for numerous fruitful discussions. A.S. acknowledges support by the APART program of the Austrian Academy of Sciences and thanks for the hospitality enjoyed during several stays at the Université Catholique de Louvain. B.P. is supported by the Fonds National de la Recherche Scientifique of Belgium.

[1] K.J. Schafer *et al.*, Phys. Rev. Lett. **70**, 1599 (1993).
[2] Baorui Yang *et al.*, Phys. Rev. Lett. **71**, 3770 (1993).
[3] R. Grobe and J.H. Eberly, Phys. Rev. Lett. **68**, 2905 (1993).
[4] D.G. Lappas *et al.*, J. Phys. B **29**, L619 (1996).
[5] J. Parker, K.T. Taylor, C.W. Clark, and S. Blodgett-Ford, J. Phys. B **29**, L33 (1996).
[6] J. Purvis *et al.*, Phys. Rev. Lett. **91**, 3943 (1993).
[7] J. Zhang and P. Lambropoulos, J. Phys. B **28**, L101 (1995).
[8] W. Reinhardt, Annu. Rev. Phys. Chem. **33**, 223 (1978).
[9] A. Kono and Sh. Hattori, Phys. Rev. A **29**, 2981 (1984).
[10] J.S. Sims and W.C. Martin, Phys. Rev. A **37**, 2259 (1988).
[11] E. Lindroth, Phys. Rev. A **49**, 4473 (1994).